Available online at www.sciencedirect.com

ScienceDirect

Procedia Structural Integrity 52 (2024) 551–559

Structural Integrity Procedia

www.elsevier.com/locate/procedia

Fracture, Damage and Structural Health Monitoring

Unsupervised Damage Localization In Composite Plates Using Lamb Waves And Conditional Generative Adversarial Networks

Marc Parziale[a], Luca Lomazzi[a], Zahra Rastin[b], Marco Giglio[a], Francesco Cadini[a,*]

[a]*Politecnico di Milano, Department of Mechanical Engineering, Milan 20156, Italy*
[b]*Independent researcher*

Abstract

Composite plates are increasingly used in several engineering fields. A common way for monitoring the health state of these structures is by analysing ultrasonic guided waves propagating in the plate. Among guided waves, Lamb waves (LWs) have shown promising diagnostic capabilities, and have been recently used for damage diagnosis in deep learning-based frameworks. However, so far, the proposed frameworks have mainly leveraged supervised algorithms, which require acquiring and labelling a large amount of data when the structure is in healthy and damaged conditions. Besides requiring much time and effort, acquiring enough data in damaged structures may not be practical in real world. Hence, this paper proposes the use of conditional generative adversarial networks (CGANs) with convolutional layers for damage localization in composite plates. As unsupervised algorithms, CGANs can be trained on LWs acquired when the structure is healthy, and do not require information about damaged states. The proposed method was validated through an experimental case study involving two different composite plates.

© 2023 The Authors. Published by Elsevier B.V.
This is an open access article under the CC BY-NC-ND license (https://creativecommons.org/licenses/by-nc-nd/4.0)
Peer-review under responsibility of Professor Ferri Aliabadi

Keywords: Structural Health Monitoring; Lamb Waves; Damage Localization; Conditional Generative Adversarial Networks

1. Introduction

Thin-walled structures find a wide application in various engineering systems, including land vehicles, aircraft, and seacraft, owing to their advantageous characteristics such as lightweight design, cost-effectiveness, and the availability of robust analysis methods (Vinson 1988). Consequently, it is essential to evaluate their structural integrity in order to detect defects at an early stage and prevent costly and hazardous failures. In recent times, significant

* Corresponding author.
E-mail address: francesco.cadini@polimi.it

2452-3216 © 2023 The Authors. Published by ELSEVIER B.V.
This is an open access article under the CC BY-NC-ND license (https://creativecommons.org/licenses/by-nc-nd/4.0)
Peer-review under responsibility of Professor Ferri Aliabadi
10.1016/j.prostr.2023.12.055

research efforts have been directed towards the development of structural health monitoring (SHM) systems that enable automated damage identification by analysing data gathered from a network of sensors installed on the structure (Farrar and Worden 2006).

Among the different techniques, two of the mostly utilized SHM frameworks exploit system vibrations or guided wave signals. In particular, vibration-based methods operate on the principle that structural damage induces modifications in the vibrational characteristics of a structure (e.g., mode shapes, natural frequencies, etc.), and several works for characterizing damage by extracting damage-related features from vibration signals have been successfully proposed (Fritzen 2005), (Goyal and Pabla 2016), (Parziale et al. 2022). However, guided wave-based techniques are better suited for detecting minor flaws and damage, compared to low-frequency vibration-based methods. This is particularly advantageous in the aircraft industry, where ensuring structural safety requires the detection of small damage. Moreover, guided wave-based methods offer benefits such as low cost, lightweight sensors, and the ability to cover large areas using few sensors (Rautela and Gopalakrishnan 2021).

Among guided waves, Lamb waves (LWs) offer interesting properties and have been shown to be promising for structural damage identification, typically using a network of piezoelectric (PZT) devices for excitation and sensing (Güemes et al. 2020). However, due to the challenges posed by the complex nature of analysing LWs, researchers have increasingly turned to machine learning algorithms to enhance the speed and accuracy of LW-based damage diagnosis (Agarwal and Mitra 2014), (Zi Zhang et al. 2020), (Mahajan and Banerjee 2022), (Lomazzi, Giglio, and Cadini 2023). Deep learning (DL) algorithms, in particular, have garnered significant attention due to their capability to automatically extract features from raw signals. Numerous DL-based approaches, mostly employing supervised algorithms, have been introduced in the literature in recent years. Among these approaches, convolutional neural networks (CNNs) have emerged as the most widely utilized (Indolia et al. 2018). As an example, in Ref. (Liu and Zhang 2020), cracks in thin aluminium plates were detected through CNNs trained on images derived from LWs. In Ref. (Rai and Mitra 2021), instead, the authors developed and evaluated a DL approach based on a multi-headed one-dimensional (1D) CNN architecture for real-time damage detection using LWs. In particular, a diverse training database was constructed and the model effectiveness in accurately predicting the condition of both experimentally generated and simulated samples was demonstrated. Another example is the work in Ref. (Wu et al. 2021), where a novel method for LW-based diagnosis of internal delamination in carbon fibre-reinforced polymers (CFRPs) exploiting CNNs and continuous wavelet transform was proposed.

Although supervised algorithms have shown good performance in detecting structural damage, they rely on a substantial amount of labelled data from both healthy and various damaged states of the target structure. This labelling process is time-consuming and labour-intensive, and acquiring a sufficient amount of damaged state data may not be practical or feasible for certain structures. To address this issue, unsupervised DL-based methods can be utilized. However, the application of these methods specifically for LW-based SHM has not been thoroughly explored and investigated in the existing literature. In particular, there are only a few published articles in this context (Rautela et al. 2022), (Rahbari et al. 2021), (Lee et al. 2022) and, to the best of the authors' knowledge, a fully unsupervised LW-based damage localization has only been studied in Ref. (Sawant et al. 2023), although a limited number of damage positions (i.e., two damage locations in a CFRP plate equipped with PZT devices) was considered.

Thus, in the present work, a novel fully unsupervised LW-based method for localizing damage in thin-walled structures is proposed. More specifically, conditional generative adversarial networks (CGANs) made of convolutional layers were implemented and used to process raw LW signals acquired on composite plates. These deep neural networks (DNNs) were trained considering system healthy states only and, unlike most of the methods proposed in the literature, they were validated against experimental data acquired on two different composite plates, where localized damage and delamination were considered.

The paper is organized as follows: in Section 2, a short description of the required theoretical background is provided, as well as an overview of the proposed approach; the case study is reported in Section 3, and concluding remarks are discussed in Section 4.

2. Methodology

The proposed unsupervised framework for structural damage localization relies on the use of a particular type of GANs, i.e., CGANs, for processing LWs. GANs consist of two neural networks, a generator and a discriminator, engaged in a competitive game (Goodfellow et al. 2014). The working principle of a GAN is schematized in Fig. 1. The generator takes a random noise vector $\boldsymbol{z}$ and converts it into realistic data $\boldsymbol{x}_f$ by mapping the noise vector to a higher-dimensionality space, usually through fully connected and/or convolutional layers. The generation of synthetic data, i.e., the fake sample, can be described by Eq. (1):

$$G(\boldsymbol{z}) \rightarrow \boldsymbol{x}_f \tag{1}$$

Instead, the discriminator acts as a binary classifier and tries to distinguish between real data and synthetic data generated by the generator, as shown in Eq. (2):

$$D(\boldsymbol{x}) \rightarrow p \in [0,1] \tag{2}$$

where $\boldsymbol{x}$ represents the input data, and p is the probability that the input is real data. GANs are trained through an adversarial process, where the generator and the discriminator play a minmax game against each other. In particular, the generator aims to fool the discriminator by generating data that the discriminator cannot distinguish from the real one. Its training loss, L_G, is calculated based on the discriminator output for the generated data, as reported in Eq. (3):

$$L_G = -\log\left(D(G(\boldsymbol{z}))\right) \tag{3}$$

The discriminator loss, instead, is calculated based on the difference between its predictions for real and fake data. It is typically defined as the sum of two cross-entropy losses, as shown in Eq. (4):

$$L_D = -\log\big(D(\boldsymbol{x})\big) - \log\left(1 - D(G(\boldsymbol{z}))\right) \tag{4}$$

where $D(\boldsymbol{x})$ represents the discriminator output when it takes real data, while $D(G(\boldsymbol{z}))$ is the discriminator output when it takes generated data $G(\boldsymbol{z})$. A limitation of traditional GANs is the lack of control over the class of generated samples. In Ref. (Mirza and Osindero 2014) this issue was addressed by introducing CGANs. CGANs are improved versions of GANs that enable the generation of samples belonging to specific classes. This is accomplished by incorporating labels into the input data of both the generator and the discriminator. The generator learns to produce samples corresponding to each class based on the provided label, while the discriminator learns to distinguish between real and fake samples of different classes.

In this paper, CGANs with convolutional layers were utilized to detect damage in thin-walled structures using PZT devices, according to the scheme shown in Fig. 2. First, different *cases* were defined based on the arrangement and number of PZT devices on the plate. In particular, each case was characterized by one PZT acting as an actuator, while the others are receivers of LWs. For example, having n PZTs, n different cases were defined, and case 1 was represented by PZT1 serving as actuator and the other $n-1$ devices acting as sensors. So, for each case, $n-1$ different actuator-sensor paths, here denoted as *classes* (or *labels*), were obtained. The signals corresponding to each class, which are represented by a sequence of N data points, were then normalized in the range $[a, b]$ and divided into smaller *sub-sequences* of m data points. That is, N/m sub-sequences were generated for each class. As a way of data augmentation, Gaussian noise was added to the signals with a defined signal-to-noise ratio δ. Then, a CGAN was associated to each case, and was trained to generate the healthy sub-sequences corresponding to the related classes. After training, signals corresponding to the different cases were acquired to characterize damage. Each signal, related to a given class of a given case, was divided in N/m sub-sequences and fed, one by one, to the discriminator part of the corresponding CGAN which, in turn, provided N/m scalars describing the probability that each sub-sequence was real (i.e., healthy) or fake (i.e., damaged). Then, the average of these values was computed and named AD_{i-j}, in which i and j are, respectively, the actuator and the sensor number in the considered path. For instance, AD_{3-4} refers to the average of the outputs of the trained discriminator in case 3 (i.e., when PZT3 is the actuator) when fed with sub-sequences received by PZT4. The same reasoning was done for the corresponding healthy state data on which the CGAN was trained, leading to a value named AH_{i-j}. A path score SP_{i-j} was then computed and defined as reported in Eq. (5):

$$SP_{i-j} = \frac{|AH_{i-j} - AD_{i-j}| + |AH_{j-i} - AD_{j-i}|}{2} \tag{5}$$

All the paths of the different PZT couples $i - j$ were considered and the corresponding path scores were computed. Finally, the plates were divided into small squares with side l, so that a grid in the area encircled by the network of PZTs was obtained. For each square, a score was computed by taking the average of the scores related to the paths intersecting the square.

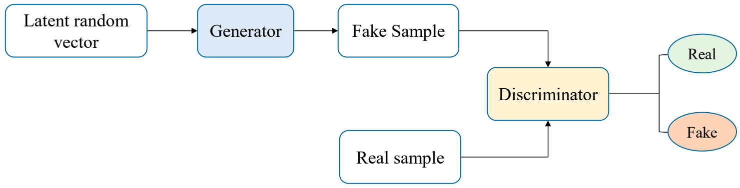

Fig. 1. Scheme of the working principle of a GAN.

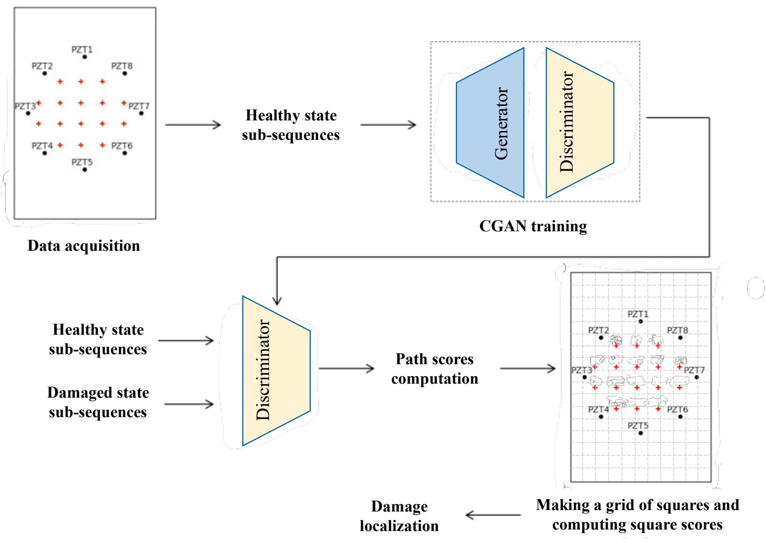

Fig. 2. Scheme of the proposed methodology for damage localization using CGANs.

3. Case study

The CGAN-based approach illustrated in the previous Section was here applied on a case study of two different 200 x 300 mm composite plates with 4 mm thickness. Plate K8 was made of Kevlar29 with 8 layers, while plate K2G4S was composed of Kevlar29 combined with S2-Glass fibre, with 4 and 8 layers, respectively, and symmetric layout $[[K]_2[G]_4]_S$. Both plates were made of woven fabric with 0º/90º orientation, and an epoxy resin AR260 with AH260 hardener from Barracuda Advanced Composites was employed. These materials were selected due to their extensive use in previous studies for validating damage localization methods based on LWs. Additionally, they are commonly employed in the fields of aeronautical and civil engineering.

Eight PZT devices provided by PI Ceramic GmBH were evenly arranged in a circular layout with a diameter of 160 mm whose centre was located at the central point of the panel. These devices have a diameter of 5 mm and a thickness of 1 mm. Fig. 3 (a) illustrates a picture of the setup installed on the K8 plate (a grid with 10 mm squares was drawn to better place the PZTs and to introduce damage).

The LWs were generated with a voltage of 10 V using a Keysight Technologies 33220A arbitrary waveform generator. Then, to amplify the signal to a level of 120 Vpp, a Khron-Hite 7602M amplifier was employed. The selected signal was a 5-cycle tone-burst with a central frequency of 150 kHz. The signal was gathered using a PicoScope 4824A oscilloscope with a sampling frequency of 4 MHz. To eliminate periodic noise, the acquired signals were filtered using a band-pass Butterworth filter spanning from 50 kHz to 250 kHz. The signal acquisition was repeated 20 times, and the final signal was determined by calculating the median value of the samples.

To create a dataset of damaged state signals, a pseudo-damage approach was adopted. This method combines the benefits of a real experimental campaign with the ability to explore a greater range of damaged scenarios (Qian et al. 2020). Scotch Vinyl Mastic Rolls 2210, commonly used for isolation and vibration damping, was utilized to simulate damage. More specifically, circular-shaped tapes with a diameter of 20 mm were cut and affixed to various positions on the surface of the panels. Sixteen different positions were analysed individually. Fig. 3 (b) illustrates the positions of the simulated damage, as well as the numbering of the PZT devices on the plates. The red plus signs indicate the centre of the circular tape piece. Note that, in addition to the pseudo-damage, also two cases of delamination resulting from real impacts were considered.

According to the methodology described in Section 2, given that 8 PTZs were installed (i.e., $n = 8$), 8 different cases were defined. For each case, the signals, corresponding to the 7 different classes (i.e., $n - 1$), were gathered and normalized in the range $[-1,1]$ (i.e., $a = -1$ and $b = 1$), and a Gaussian noise with a signal-to-noise ratio $\delta = 20\ dB$ was added as data augmentation technique. Subsequently, each signal was divided into 1000 sub-sequences of 128 data points (i.e., $N = 128000$ and $m = 128$). Then, 8 CGANs, one for each case, were trained on the healthy sub-sequences corresponding to the different classes. The hidden architecture of the generator part of these networks consisted of a dense layer, three 1D convolutional layers and two up-sampling layers placed after the first two 1D convolutional ones. The dense layer was made of 2048 neurons, and its output was then reshaped into a size of 32 x 64 to be fed to the first 1D convolutional layer that consisted of 32 filters, while the second and third 1D convolutional layers were made of 16 and 1 filters, respectively. All convolutional layers had filters with a size of 2, stride 1, and same padding. Moreover, after the first two convolutional layers, a leaky rectified linear unit (ReLU) (with parameter $\alpha = 0.01$) (Xu et al. 2015) was adopted while, for the last one, a hyperbolic tangent was used. For what concerns the up-sampling layers, the up-sampling factor was set to 2. During the training, the input of the generator was a vector with size 64 x 1 whose elements were sampled from a gaussian distribution with mean $\mu = 0$ and standard deviation $\sigma = 1$. Regarding the discriminator part, its hidden architecture was composed of three 1D convolutional layers and one dense layer. In particular, the convolutional layers had 1, 16 and 32 filters, respectively, with a size of 2, stride 1, and same padding. The dense layer, instead, was made of 1 neuron. Moreover, a leaky ReLU was applied after the three convolutional layers (with parameter $\alpha = 0.01$), and a sigmoid function was used after the dense one. For training the CGANs, a binary cross-entropy was employed as loss function and the Adam optimizer algorithm was used (with learning rate $\eta = 0.01$, parameters $\beta_1 = 0.90$, $\beta_2 = 0.99$ and $\varepsilon = 1 \cdot 10^{-7}$) (Zijun Zhang 2019).

Once the CGANs were trained, the discriminator part was used to localize the damages in the plate by assigning a score to the path between each pair of PZT devices, making a grid, and calculating a score for each of the squares in the grid. In particular, a grid of squares with side $l = 30\ mm$ was chosen for this purpose by trial-and-error. Indeed, this value leads, for the given PZT devices layout, to an optimal number of actuator-sensor paths cutting the squares. The damage localization results for the damage positions D1, D4, D6, D8, D14 and D15 are reported in Fig. 4 and Fig. 5, where the white circumference denotes the pseudo-damage and the red cross indicates the predicted damage location (i.e., where the computed score is higher). Note that, to obtain those images, the obtained scores were normalized between $[0, 1]$ and then interpolated with a Hanning function interpolation method to get a smoother representation. The Euclidean distance between the true and predicted damage location was computed for the mentioned damaged scenarios to evaluate the localization accuracy. The obtained values are shown in Table 1. What arose is that, in both plates, the damage localization error was lower than 1.5 mm for the damage location D4, reaching the highest values at position D6 for the K8 plate and D8 for the K2G4S plate, where the error was around 33 mm and 23 mm, respectively. In all the other scenarios, the error was lower than 6 mm.

Furthermore, the generalization capabilities of the method were evaluated by localizing damage after subjecting the plates to a low velocity impact of 50 J at damage position D11. The results reported in Fig. 6 (position D11 highlighted with a white circle) show how the prediction (higher score value represented with a red cross) was significantly close to the impact position, i.e., where damage is expected to start from, for the K8 plate, while for the hybrid plate the approach was less accurate.

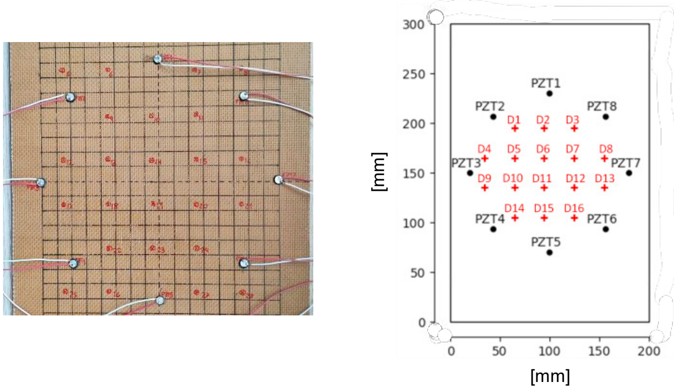

(a) (b)

Fig. 3. Picture of the K8 plate with the PZTs installed (a) and the considered damage positions highlighted with red plus signs together with the PZTs numbering (b).

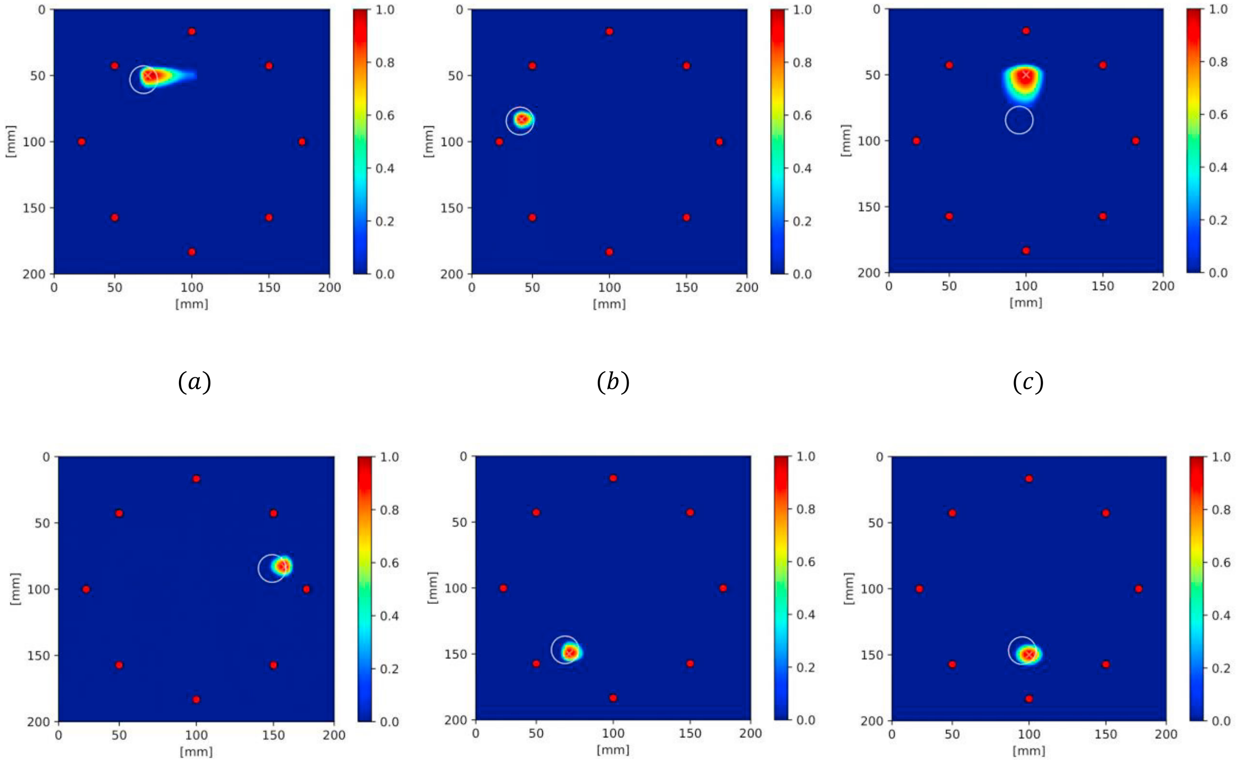

(a) (b) (c)

(d) (e) (f)

Fig. 4. Kevlar panel (K8) localization results: position D1 (a), position D4 (b), position D6 (c), position D8 (d), position D14 (e), position D15 (f); true damage location highlighted with a white circumference and the predicted one (where the score is higher) with a red cross.

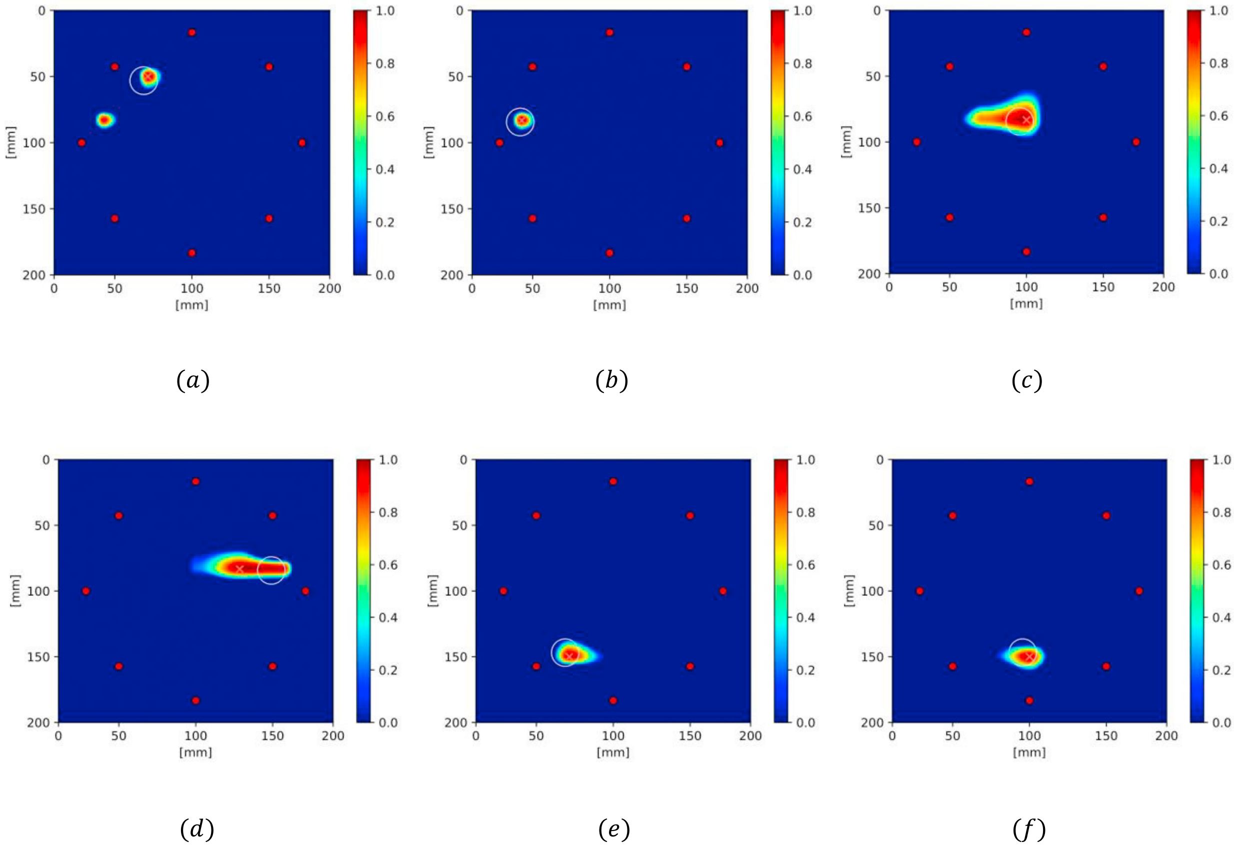

Fig. 5. Hybrid panel (K2G4S) localization results: position D1 (a), position D4 (b), position D6 (c), position D8 (d), position D14 (e), position D15 (f); true damage location highlighted with a white circumference and the predicted one (where the score is higher) with a red cross.

Table 1. Distance between the real pseudo-damage centre and the predicted one.

Material	Position	Distance $[mm]$
K8	D1	4.242
	D4	1.415
	D6	33.376
	D8	9.055
	D14	4.242
	D15	5.831
K2G4S	D1	4.243
	D4	1.414
	D6	5.099
	D8	23.021
	D14	4.243
	D15	5.831

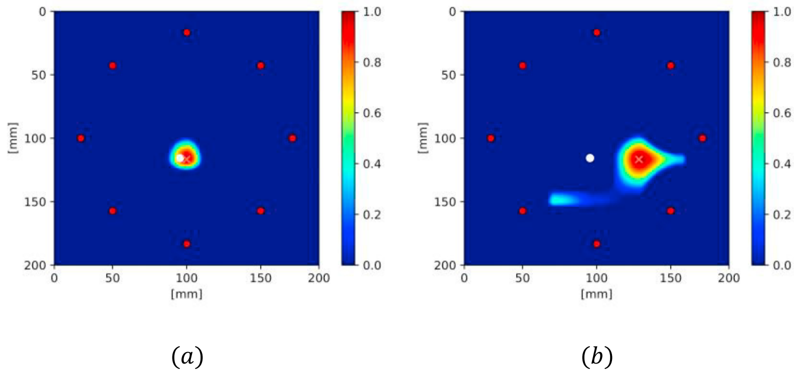

Fig. 6. Impact damage localization results: Kevlar panel (K8) (a), hybrid panel (K2G4S) (b); true damage location (D11) highlighted with a white circle and the predicted one (where the score is higher) with a red cross.

4. Conclusions

A novel LW-based unsupervised damage localization method exploiting CGANs has been proposed and applied to two experimental composite plates made of Kevlar and Kevlar combined with glass fibre, respectively. In particular, the employed method can localize damage by training the networks with healthy data only, thus dealing with the issue related to the need of labelled data. The approach has been tested considering pseudo-damage in six different damage locations, showing good accuracy for both plates. Moreover, in order to also evaluate the algorithm generalization capabilities, a damage localization of low velocity impacts has been assessed, exhibiting remarkable accuracy for the Kevlar plate, and satisfactory results for the hybrid plate.

Future work may involve characterizing damage under changing environmental conditions and evaluating the performance of the proposed method against more complex damaged scenarios, such as the presence of multiple damage simultaneously.

References

Agarwal, Sushant, and Mira Mitra. 2014. "Lamb Wave Based Automatic Damage Detection Using Matching Pursuit and Machine Learning." *Smart Materials and Structures* 23(8): 085012. https://iopscience.iop.org/article/10.1088/0964-1726/23/8/085012 (May 24, 2023).

Farrar, Charles R., and Keith Worden. 2006. "An Introduction to Structural Health Monitoring." *Philosophical Transactions of the Royal Society A: Mathematical, Physical and Engineering Sciences* 365(1851): 303–15. https://royalsocietypublishing.org/doi/10.1098/rsta.2006.1928 (May 24, 2023).

Fritzen, Claus Peter. 2005. "Vibration-Based Structural Health Monitoring – Concepts and Applications." *Key Engineering Materials* 293–294: 3–20. https://www.scientific.net/KEM.293-294.3 (May 24, 2023).

Goodfellow, Ian et al. 2014. "Generative Adversarial Networks." *Communications of the ACM* 63(11): 139–44. https://arxiv.org/abs/1406.2661v1 (May 25, 2023).

Goyal, D., and B. S. Pabla. 2016. "The Vibration Monitoring Methods and Signal Processing Techniques for Structural Health Monitoring: A Review." *Archives of Computational Methods in Engineering* 23(4): 585–94. https://link.springer.com/article/10.1007/s11831-015-9145-0 (May 24, 2023).

Güemes, Alfredo, Antonio Fernandez-Lopez, Angel Renato Pozo, and Julián Sierra-Pérez. 2020. "Structural Health Monitoring for Advanced Composite Structures: A Review." *Journal of Composites Science 2020, Vol. 4, Page 13* 4(1): 13. https://www.mdpi.com/2504-477X/4/1/13/htm (May 24, 2023).

Indolia, Sakshi, Anil Kumar Goswami, S. P. Mishra, and Pooja Asopa. 2018. "Conceptual Understanding of Convolutional Neural Network- A Deep Learning Approach." *Procedia Computer Science* 132: 679–88. https://doi.org/10.1016/j.procs.2018.05.069.

Lee, Hyunseong et al. 2022. "Automated Fatigue Damage Detection and Classification Technique for Composite Structures Using Lamb Waves and Deep Autoencoder." *Mechanical Systems and Signal Processing* 163: 108148.

Liu, Heng, and Yunfeng Zhang. 2020. "Deep Learning Based Crack Damage Detection Technique for Thin Plate Structures Using Guided Lamb

Wave Signals." *Smart Materials and Structures* 29(1).

Lomazzi, Luca, Marco Giglio, and Francesco Cadini. 2023. "Towards a Deep Learning-Based Unified Approach for Structural Damage Detection, Localisation and Quantification." *Engineering Applications of Artificial Intelligence* 121: 106003.

Mahajan, Harsh, and Sauvik Banerjee. 2022. "A Machine Learning Framework for Guided Wave-Based Damage Detection of Rail Head Using Surface-Bonded Piezo-Electric Wafer Transducers." *Machine Learning with Applications* 7(November 2021): 100216. https://doi.org/10.1016/j.mlwa.2021.100216.

Mirza, Mehdi, and Simon Osindero. 2014. "Conditional Generative Adversarial Nets." https://arxiv.org/abs/1411.1784v1 (May 25, 2023).

Parziale, Marc, Luca Lomazzi, Marco Giglio, and Francesco Cadini. 2022. "Vibration-Based Structural Health Monitoring Exploiting a Combination of Convolutional Neural Networks and Autoencoders for Temperature Effects Neutralization." *Structural Control and Health Monitoring* 29(11): e3076. https://onlinelibrary.wiley.com/doi/full/10.1002/stc.3076 (May 24, 2023).

Qian, Cheng et al. 2020. "Application of Artificial Neural Networks for Quantitative Damage Detection in Unidirectional Composite Structures Based on Lamb Waves." *Advances in Mechanical Engineering* 12(3). https://journals.sagepub.com/doi/full/10.1177/1687814020914732 (May 26, 2023).

Rahbari, Amirhossein, Marc Rébillat, Nazih Mechbal, and Stephane Canu. 2021. "Unsupervised Damage Clustering in Complex Aeronautical Composite Structures Monitored by Lamb Waves: An Inductive Approach." *Engineering Applications of Artificial Intelligence* 97: 104099.

Rai, Akshay, and Mira Mitra. 2021. "Lamb Wave Based Damage Detection in Metallic Plates Using Multi-Headed 1-Dimensional Convolutional Neural Network." *Smart Materials and Structures* 30(3): 035010. https://iopscience.iop.org/article/10.1088/1361-665X/abdd00 (October 15, 2022).

Rautela, Mahindra, and S. Gopalakrishnan. 2021. "Ultrasonic Guided Wave Based Structural Damage Detection and Localization Using Model Assisted Convolutional and Recurrent Neural Networks." *Expert Systems with Applications* 167: 114189.

Rautela, Mahindra, J. Senthilnath, Ernesto Monaco, and S. Gopalakrishnan. 2022. "Delamination Prediction in Composite Panels Using Unsupervised-Feature Learning Methods with Wavelet-Enhanced Guided Wave Representations." *Composite Structures* 291: 115579.

Sawant, Shruti, Amit Sethi, Sauvik Banerjee, and Siddharth Tallur. 2023. "Unsupervised Learning Framework for Temperature Compensated Damage Identification and Localization in Ultrasonic Guided Wave SHM with Transfer Learning." *Ultrasonics* 130. https://pubmed.ncbi.nlm.nih.gov/36681008/ (May 24, 2023).

Vinson, Jack R. 1988. "The Behavior of Thin Walled Structures: Beams, Plates, and Shells." *The Behavior of Thin Walled Structures: Beams, Plates, and Shells*.

Wu, Jun et al. 2021. "Lamb Wave-Based Damage Detection of Composite Structures Using Deep Convolutional Neural Network and Continuous Wavelet Transform." *Composite Structures* 276(August): 114590. https://doi.org/10.1016/j.compstruct.2021.114590.

Xu, Bing et al. 2015. "Empirical Evaluation of Rectified Activations in Convolutional Network." https://arxiv.org/abs/1505.00853v2 (May 26, 2023).

Zhang, Zi, Hong Pan, Xingyu Wang, and Zhibin Lin. 2020. "Machine Learning-Enriched Lamb Wave Approaches for Automated Damage Detection." *Sensors 2020, Vol. 20, Page 1790* 20(6): 1790. https://www.mdpi.com/1424-8220/20/6/1790/htm (May 24, 2023).

Zhang, Zijun. 2019. "Improved Adam Optimizer for Deep Neural Networks." *2018 IEEE/ACM 26th International Symposium on Quality of Service, IWQoS 2018*.